PAPER • OPEN ACCESS

Si-atoms substitutions effects on the electronic and optical properties of coronene and ovalene

New Journal of Physics
The open access journal at the forefront of physics

Deutsche Physikalische Gesellschaft DPG
IOP Institute of Physics

Published in partnership with: Deutsche Physikalische Gesellschaft and the Institute of Physics

OPEN ACCESS

RECEIVED
13 April 2018

REVISED
11 September 2018

ACCEPTED FOR PUBLICATION
12 October 2018

PUBLISHED
6 November 2018

PAPER

Si-atoms substitutions effects on the electronic and optical properties of coronene and ovalene

P Mocci[1,2], **R Cardia**[1] **and G Cappellini**[1]

Department of Physics, University of Cagliari, Monserrato (CA), Italy
[1] Present address: Department of Physics, University of Cagliari, Monserrato (CA), Italy.
[2] Author to whom any correspondence should be addressed.

E-mail: paola.mocci@dsf.unica.it, roberto.cardia@dsf.unica.it and giancarlo.cappellini@dsf.unica.it

Keywords: 2D systems, clusters, time dependent density functional theory (TDDFT)

Abstract

We report a computational comparative study of the ground and excited states properties of graphene nanoribbons, analyzing the case of coronene ($C_{24}H_{12}$) and ovalene ($C_{32}H_{14}$) and their silicon-atoms substituted counterparts with single, double and triple atomic insertions. We used density functional theory (DFT) and time-dependent DFT to quantify the effects on the electronic and optical properties as a result of the chemical modifications. In particular, we compared ground-state total energies, electron affinities, ionization energies, fundamental gaps and optical absorption spectra, between the original systems and each substituted one. For both the molecules, we observed a general reduction of the fundamental gap after chemical modification. Concerning the optical properties, therefore, we observed a redshift of the optical onset in all the cases; in particular, we have found that, in one ovalene and coronene trimer-substituted configuration, the absorption edge takes place in the IR.

1. Introduction

The importance of 2D systems (like graphene and silicene) [1, 2] has rapidly and highly increased during the last years and is now in incessant development, thanks to their advantageous electronic, mechanical and optical properties (planar feature, flexibility, resistance....). These materials are, in fact, considered among the most promising candidates for dozens of different technological optoelectronic devices. In the contest of optoelectronic, silicon is one of the most useful elements to mankind, covering a considerable position for several reasons, especially for those linked to its electronic and optical properties that can be easily modulated and controlled [3]. Moreover, optoelectronic, that is a branch based on the study and the operation of electronic devices that produce, detect, and control light, actually is an esteemed and rapidly growing field [4]: recently, 2D materials, carbon nanotubes, and semiconductor quantum dots are elements of great attention thanks to their potential use in nano and optoelectronic devices. In this field, the role of polycyclic aromatic hydrocarbons (PAHs) in their crystalline and thin-film state has largely increased. In fact, they are employed as active elements in several optoelectronic applications, ranging from light-emitting diodes, solar arrays, transparent and flexible displays to organic thin-film field-effect transistors and liquid crystals. Among them, the 'Circumacenes' (coronene, ovalene, circumanthracene, circumtetracene, and circumpentacene) have recently aroused scientific interest [5, 6]. These systems are here considered for their interesting and promising properties: they are the smallest in size among the Circumacenes, showing a nanometric dimension with a characteristic symmetric structure and a planar geometry, as figure 1 shows. Furthermore, these molecules are of wide interest in many contests of research (from condensed matter physics to astrochemistry) and also for solid state applications [7].

We selected the coronene (also known as 'superbenzene'), which is a symmetric molecule composed by the union of six benzene rings (with chemical formula $C_{24}H_{12}$) and ovalene ($C_{32}H_{14}$), that can be obtained from coronene by the addition of three benzene rings. The first one occurs in nature as the very rare mineral carpathite, that is characterized by flakes of pure coronene embedded in sedimentary rock and it can be synthesize through the petroleum-refining process of hydrocracking [8]; the second one is a reddish-orange compound that can be likewise producted. These small-size molecules, with respect to polymers, offer several

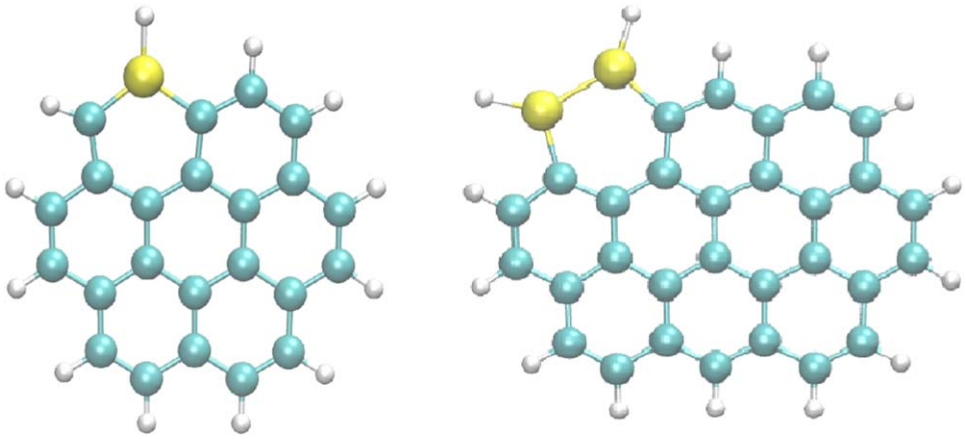

Figure 1. Coronene (left) and ovalene (right) with Si-atoms substitutions. C atoms are in cian color, while Si atoms are reported in yellow and H atoms on the boundaries in white.

advantages, such as the easy purification through various techniques and the possibility to be tractable by both evaporation and solution-processing methods [5].

The principal aim of this work consists in the study of the effects that silicon-atoms substitutions induce in coronene and in ovalene molecules considering their electronic and optical properties. We have evaluated single, double and triple-atom substitutions of silicon into these molecules, analyzing their consequences. One of the goals of this work in fact is the analysis of finite-size effects in the electronic and optical properties of the nanometric portions of graphene compounds after silicon-atoms substitutions, with possible subsequent extentions to their infinite counterparts and in connection with other previous studies [9–11]. Through the density functional theory (DFT) technique [12] we have computed and compared the electronic properties of the systems under study (e.g. electron affinities, ionization energies, quasi-particle (QP) gaps) within a gaussian-based localized orbital all-electrons scheme. We have also calculated the optical absorption spectra of the above clusters via the time dependent DFT (TDDFT) scheme[13], examining the differences as a function of different silicon substitutions, trying to find possible trends. Moreover, a connection of the results with existing outcomes of previous theoretical and experimental works will be considered.

2. Computational methods

Carrying on previous works [5, 6], we have performed geometry optimizations using the hybrid exchange-correlation functional B3LYP [14–16], combined with the $6-31G^*$ basis-set, a valence double-ζ set augmented with *d* polarization functions for each atom. We used the B3LYP exchange-correlation potential, since with respect to other possible choices (e.g. the Perdew–Burke–Ernzerhof [17]), it has been proved to reproduce better results for different families of PAHs molecules, whether for ground-state or the excited properties [5, 18–20]. Geometry optimizations have been obtained using tight convergence criteria, specified by maximum and root mean square gradient thresholds of 1.5×10^{-5} and 1.0×10^{-5}, respectively, and maximum and root mean square thresholds of the Cartesian step respectively of 6.0×10^{-5} and 4.0×10^{-5}; all the values are given in atomic units. All the molecular relaxations have been computed without symmetry constraints. At the optimized geometry of the neutral pure molecules, we have evaluated the vertical ionization energies (IE_V) and the electron affinities (EA_V). This allows the calculation of the QP gap (also known as 'fundamental gap'), which is rigorously defined in the ΔSCF scheme as [21, 22]:

$$E_{\mathrm{gap}} = \mathrm{IE}_V - \mathrm{EA}_V = (E^0_{N-1} - E^0_N) - (E^0_N - E^0_{N+1}), \tag{1}$$

where E_N indicates the ground-state total energy of the *N*-electron system. According to this method, we have computed vertical transitions, considering the differences between the ground-state total energy of the neutral system, E^0_N, and the energies of the charged species (the anion E^0_{N+1} and the cation E^0_{N-1}, respectively), calculated at the neutral geometry. To obtain the electronic absorption spectra in the visible/near-UV regions, we performed TDDFT calculations, using the frequency space implementation present in the computational package, at the same level $B3LYP/6-31G^*$ set for the electronic ground-state. According to this method, the poles of the linear response function correspond to the vertical excitation energies and the pole strengths represent the oscillator strengths [23]. In particular, from the knowledge of the first optically active transition, E_{opt}, we could estimate the exciton binding energy expressed by the difference $E_{\mathrm{bind}} = E_{\mathrm{gap}} - E_{\mathrm{opt}}$. It is well

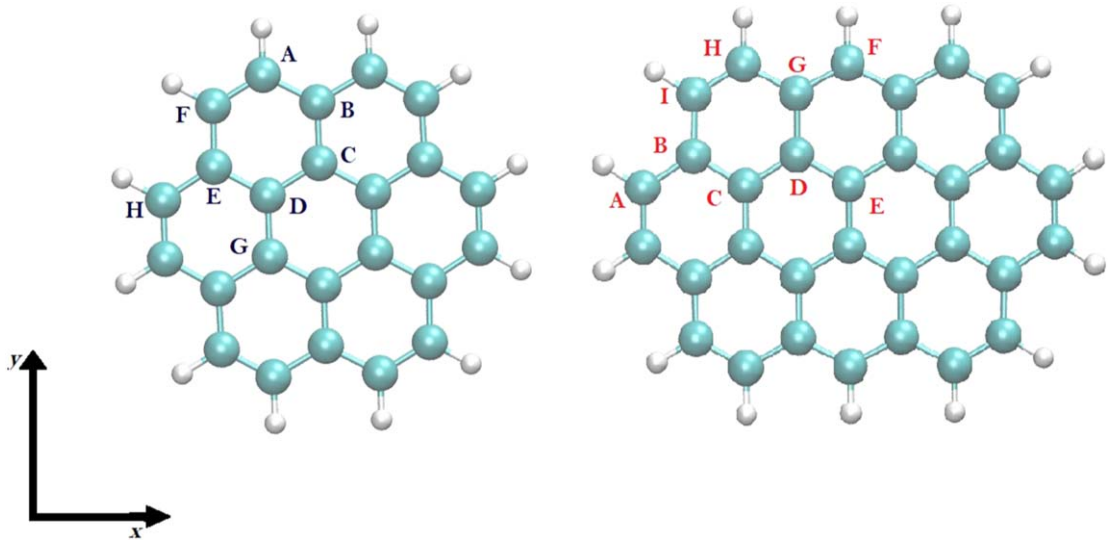

Figure 2. Coronene and ovalene molecules. The C atoms selected to be replaced by Si atoms are indicated by letters from A to H for coronene (left), while from A to I for ovalene (right). Dimers and trimers are composed by the union of the neighbor individual ones.

known that the technique here used to evaluate the exciton-binding energy is an approximated method to obtain that observable. However, in the case of systematic studies on several molecules, this scheme turns out to be particularly useful and straightforward in order to obtain the correct trend and the order of magnitude of the observables. This without recurring to the use of most demanding computational techniques [24, 25]. All the calculations have been performed using NWChem [26] computational package. This computational package is based on a numerical resolution of the Khon–Sham equations after a DFT Hamiltonian [12]. The exchange and correlation effects are treated resorting to a particular functional inserted in the Hamiltonian after the B3LYP scheme [14–16].

3. Results and discussion

3.1. Configurations with silicon atoms substitutions

The possible non-equivalent substitutions of silicon atoms, based on the molecular symmetries, are the following (see figure 2):

- 6 (9) configurations after single Si-atom insertions in coronene (ovalene);
- 4 (9) configurations after double Si-atom insertions in coronene (ovalene);
- 4 (10) configurations after triple Si-atom insertions in coronene (ovalene).

Moreover, in the case of coronene, the configurations number is reduced from 6 to 3 for single substitutions, because of the equivalence between A–F, B–E and C–D atoms (see figure 2). Considering the ovalene structure, the addition of three benzene rings implies an increase of possible configurations number, involving a reduction of the molecular symmetry. Among all these arrangements, in the following lines, we have presented only one system for each substitution, for both coronene and ovalene. The selection criterion is based on the evaluation of the energy stability of the substituted clusters. In particular, we have found that, from the energetic point of view, the most favorable configurations are the following ones: for single substitutions the atom placed in A (H) position in the case of coronene (ovalene), for the double insertions the dimer composed by A–F (H–I) atoms for coronene (ovalene) and finally for the triple substitutions the trimer formed by the union of B–A–F (H–I–B) atoms for coronene (ovalene). Aside from these particular cases here analyzed in detail, all the optical absorption for all the possible substitutions are reported in the appendix.

In general, the energy stability tends to decrease, in the substituted systems with silicon atoms, from the external to the innermost molecular regions: this means that, the most stable configurations are potentially those in which the substitutional site is placed in the peripheral molecular areas (for a more in-depth explanation see tables A1 and A2 in the appendix). A possible physical motivation of this occurrence is that in the outer regions there are less constraints which colud bound the deformations after Si-atoms insertions. This fact could cause larger total energies when the insertions are performed in the periphery of the cluster: silicon has, in fact, a larger

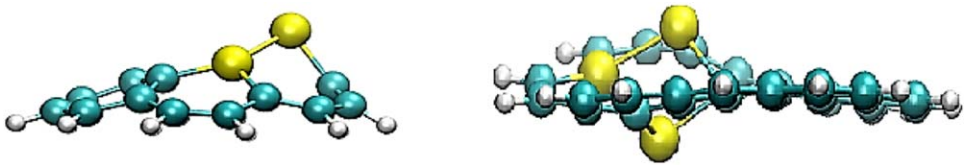

Figure 3. Lateral view of coronene (left) and ovalene (right) molecules with the Si-trimer substitution which do not preserve the planar geometry, typical of their pure parents as shown in figure 1.

Table 1. Ground-state total energies, E_0^n, for coronene and ovalene substituted molecules (single, dimer and trimer substitution).The percentage deviation, Δ, passing from coronene to ovalene corresponding system is also indicated.

Ground-state total energies		
	E_0^n (keV)	Δ(%)
Coronene	−25.1	—
Single-sub	−31.9	—
Double-sub	−38.8	—
Triple-sub	−45.6	—
Ovalene	−33.4	+33%
Single-sub	−40.2	+26%
Double-sub	−47.1	+21.4%
Triple-sub	−53.9	+18.2%

covalent radius than carbon and therefore, if inserted in a C matrix can provoke distortions of the original structure. The configurations of substituted species were found to preserve the planar geometry of their parent molecules, after single and double Si-atoms inclusions: the deformations are, in these cases, planar and localized, close to the point in which the insertion is made. On the contrary, for both coronene and ovalene, the insertion of a trimer, in some case, breaks their planar appearance (see figure 3), in which are reproduced the substitution of the trimer composed by the atoms placed on the central ring for coronene and by the atoms B C D for ovalene. In these cases the distortions are extended in the 'out-of-plane' directions. This effect seems to be more pronounced for ovalene than for coronene, as demonstrated by the variation of the interatomic bonds connecting Si–C atoms. Details of the silicon insertions on the morphological properties have been given in a previous work [27].

From DFT calculations (see table 1), we recorded that ovalene ground-state total energy (−33.4 keV) exceeds the 33% that of coronene (−25.1 keV): this is a consequence of the larger number of electrons. The increase in the energy stability shown by substituted-ovalene configurations with respect to the corresponding substituted-coronene are of about 26%, 21%, 18% for single, double and triple insertions, respectively. Exploring the effects of silicon insertions, we have recorded that the ground-state energy increases, in absolute value, in the range between ∼27% and 82% (∼20%–61%) comparing the coronene (ovalene) and its modified configurations, going from single to triple substitutions, respectively.

This means that in the case of each substituted configuration, the effects of silicon inclusions imply an increase of the energy stability with respect the corresponding original parent and in addition, this result is larger for coronene as compared to ovalene. In this work we limited our study on the linear inclusions only, even if it is well known that these structures, which could be obtained by non-equilibrium processes (e.g. synthesis process with use of plasma [28]) are metastable.

3.2. Electronic properties

Tables 1–3 report the computed data for ground and excited states of coronene and ovalene molecules and their selected substituted configurations, as previous indicated. The percentage deviation (Δ) is calculated with respect to coronene.

We first considered the comparison between the original molecules, indicating the percentage variation for each observable, passing from coronene to ovalene and then for their substituted geometries. In relation to ground-state total energies, all ovalene configurations show deeper energies than those of coronene (that is an

Table 2. Electron affinity (EA_V), ionization energy (IE_V) and fundamental gap (E_{gap}) for coronene and ovalene substituted molecules (with single, dimer and trimer substitutions). The percentage deviation, Δ, passing from coronene to ovalene corresponding system is also reported.

	EA_V	IE_V	E_{gap}
Coronene	0.03	6.85	6.82
Single-sub.	0.11	6.43	6.32
Dimer-sub.	0.31	6.37	6.06
Trimer-sub.	0.6	6.24	5.64
Ovalene	0.77 −	6.18 (−9.8%)	5.38 (−20.8%)
Single-sub.	0.80(+600%)	5.95 (−7.5%)	5.15 (−18.5%)
Dimer-sub.	0.81 (+161%)	5.96(−6.4%)	5.14 (−15.2%)
Trimer-sub.	0.87 (+45%)	5.80 (−7%)	4.93 (−12.5%)

Table 3. HOMO–LUMO gap Δ_{HL} for coronene and ovalene substituted molecules (with single, dimer and trimer substitution) with indicated also the value of the percentage deviation Δ.

HOMO–LUMO gap		
	Δ_{HL} (eV)	Δ(%)
Coronene	4.03	—
Single-sub	3.59	—
Double-sub	3.66	—
Triple-sub	3.61	—
Ovalene	3.05	−24%
Single-sub	2.89	−19%
Double-sub	2.90	−21%
Triple-sub	2.91	−19%

Table 4. Theoretical and experimental data (in brackets after literature) for the electron affinity (EA_V) and the ionization energy (IE_V) for coronene and ovalene, as obtained after [30, 31], respectively.

	EA_V	IE_V
Coronene	0.38 (0.47 ± 0.090)	7.08 (7.29 ± 0.03)
Ovalene	1.10 (–)	6.41 (6.71)

increase, in absolute value, of the ground-state total energy (E_0^n) and this is a consequence of the increase in the number of electrons). The ovalene vertical electron affinity, EA_V, is ∼26 times larger as compared to the coronene one, while the situation is reversed for the ionization energy, IE_V,which results larger by ∼9.8% for coronene (6.85 eV) than ovalene (6.18 eV). As a consequence, the corresponding QP gaps (E_{gap}) are of the same order of magnitude, 6.82 (5.40) eV for coronene (ovalene), respectively. Only in the case of coronene vertical electron affinity, EA_V, the calculation has been performed using the $6-31+G^*$ basis-set (which includes the atomic diffuse functions), instead of the $6-31G^*$, to heal an anomaly in the value obtained for that observable [29], with the resultant value of $EA_V = 0.39$eV. We have decided to report in table 2 all the data, calculated for coherence with the same basis-set ($6-31G^*$) but a connection with the available theoretical/experimental data for the coronene EA_V needed the implementation of the diffuse functions included in the $6-31+G^*$ basis-set (see table 4). Figure 4 shows some of the same data through a diagrammatic plot for coronene and ovalene[3]. Finally, the HOMO–LUMO gap, Δ_{HL}, is reduced by ∼24% from coronene (4.03 eV) to ovalene (3.05 eV).

We now consider the effects induced by Si-atoms substitutions, switching from coronene on ovalene and then the same effects passing from the pure molecule to the substituted ones. As shown in table 2, there is an increase in the vertical electron affinities, going from coronene to ovalene, for each type of substitution (from

[3] The representation by figure 4 takes into account the coronene $EA_V = 0.39$ as obtained with the $6-31+G^*$ basis-set, to make possible a more consistent connection with the data from the literature reported in table 4. For the optical onsets and exciton binding energies see the dedicated section.

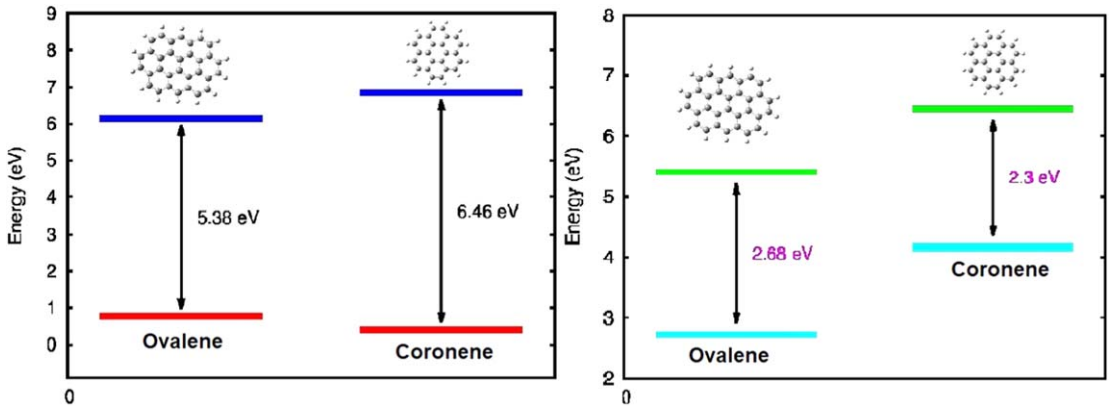

Figure 4. (Left) Vertical electron affinities (red lines), vertical ionization energies (blue lines) and fundamental gaps (black arrows) for ovalene (left) and coronene (right). (Right) Fundamental gaps (green lines), optical onsets (light blue lines) and exciton binding energies (black arrows) for ovalene (left) and coronene (right).

45% to 600%), while, on the other hand, the vertical ionization energies and the fundamental gaps show a general decrease (of about 7% and from ∼12% to 18%, respectively). The deviations of the HOMO–LUMO gaps (see table 3) for the ovalene-substituted systems with the corresponding coronene ones remain almost constant (the reduction oscillates around 19%–21%). The analysis of the substitutional effects on the electronic properties, with respect to its original compound, follows.

We have found that for coronene (ovalene) vertical electron affinity the variation range is between ∼+300%–1900% (4%–13%), considering the minimum and the maximum value. For the vertical ionization energy, we recorded a decrease included in the range of ∼6%–9% (∼3%–5%) for coronene (ovalene). For the fundamental gap the reduction with respect to the corresponding original parent is of about ∼7%–10% (∼4.5%–8.5%) in the case of coronene (ovalene). Finally, for what concerns the HOMO–LUMO gaps (see table 3), we have calculated that the percentage reduction oscillates around the average value of ∼–10% for coronene and ∼–5% for ovalene, considering all the substitutions, respectively.

Moreover, table 4 reports the theoretical and experimental data (in brackets) for the vertical electron affinity (EA_V) and the vertical ionization energy (IE_V) of coronene and ovalene, as obtained by [30, 31], respectively. For the electron affinities, we have found that the theoretical (experimental) values differ from our calculated data by ∼ +2%(−17%) and by +30% for coronene and ovalene, respectively. While for the ionization energies we recorded theoretical (experimental) values larger by +3.2% (+6%) and +3.6%(+8%) for coronene and ovalene, respectively.

3.3. Optical properties

For the optical absorption concerning the substituted systems we have performed the calculations for all the possible substitutions considered in the present work. The overall data are reported in the appendix with a corresponding comment. In the following lines we analyze in detail the optical properties of only the substituted systems which we have selected with the criterion of the minimum ground-state total energy (see the dedicated subsection 'Configurations with silicon atoms substitutions'). Figure 5 shows the comparison between the pure molecules absorption spectra, while figures 6 and 7 represent the absorption spectra for coronene and ovalene in the visible/near-UV region up to 5.5 eV, as given by B3LYP/6 − 31G^* TDDFT calculations, for each substituted configuration with the corresponding original counterpart.

Table 5 reports the wavelengths of the main peaks appaering in the cross-section of coronene and ovalene here calculated with the dominant peak in the experimental absorbance of graphene after [32]. While coronene and ovalene, considered as nanometric portions of infinite graphene sheets, show spectra characterized by a rich structure with different peaks, the experimental absorbance of graphene is distinguished by the presence of a single dominant structure, quite broaden, which covers roughly the same wavelength range. In fact, it presents only one absorption peak localized around 275 nm and it is also characterized by a steep rise for wavelengths shorter than 250 nm.

On the other hand coronene and ovalene present both dominant peak at larger wavelengths, namely 300 and 340 nm. Table 6 reports the computed data for the coronene and ovalene optical properties and those of their substituted systems. From these results it is possible to note that a general reduction of the optical onsets (E_{opt}) and of the main peaks between the substituted-systems (for single, dimer and trimer insertions) and their original molecule takes place as a function of the number of the inserted silicon atoms, either for coronene and ovalene. In particular, in the case of coronene (ovalene) the optical onset reduction oscillates in the range

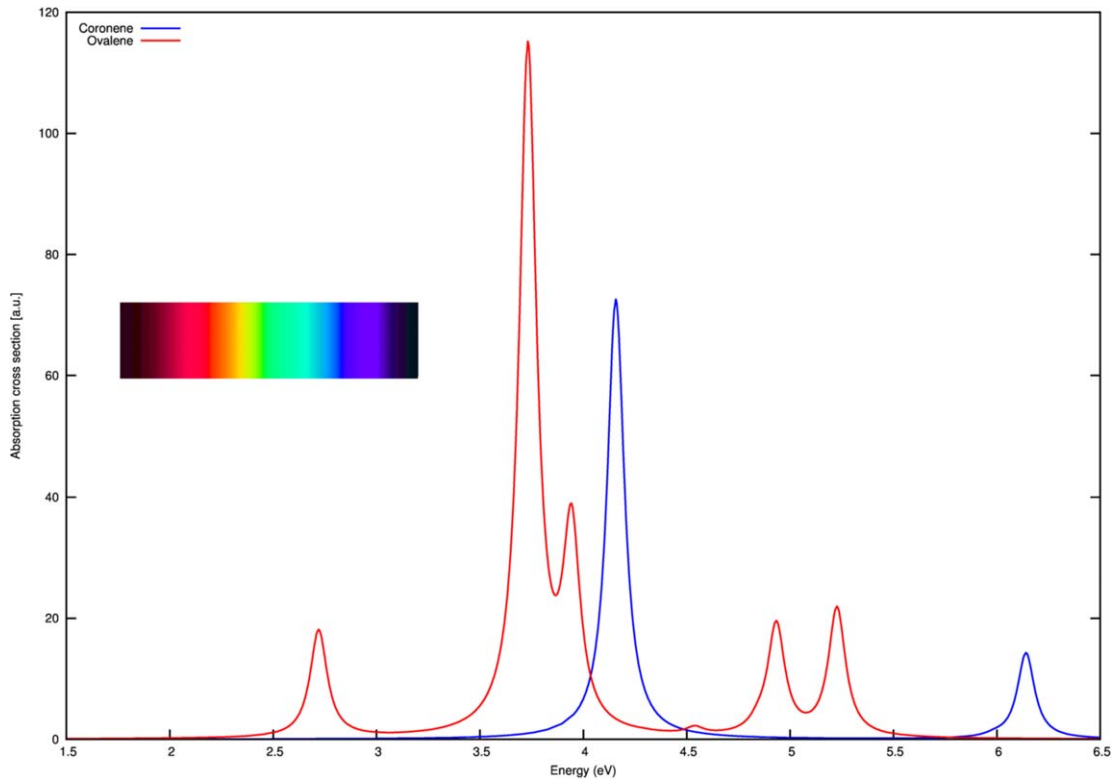

Figure 5. Absorption spectra of coronene (blue curve) and ovalene (red curve) after present calculations. The visible range is also reported.

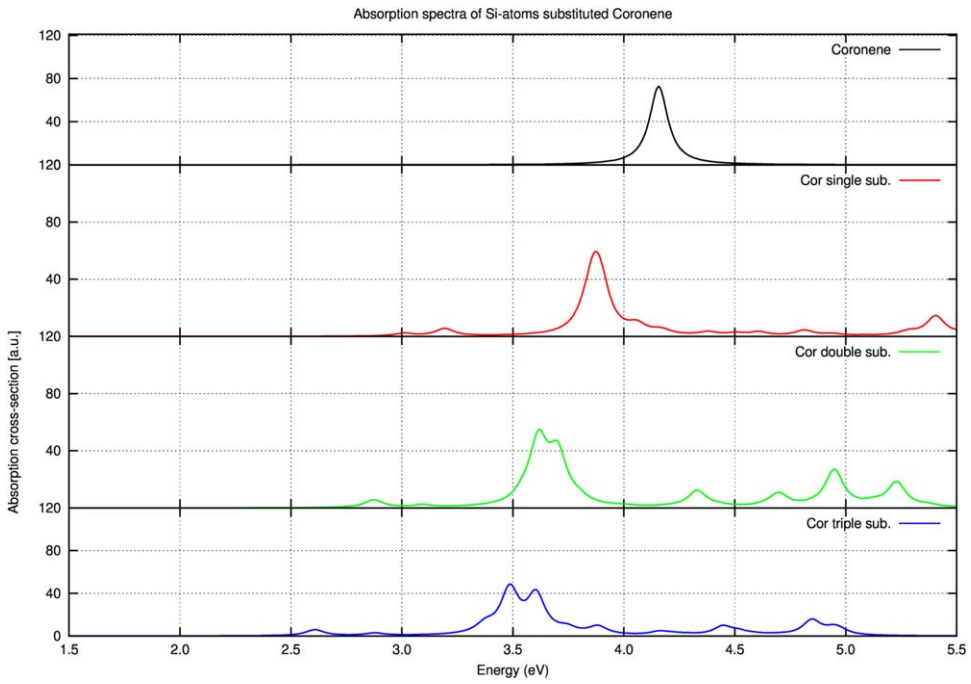

Figure 6. Absorption cross-sections [a.u.] of the selected coronene substituted systems (with single, double and triple Si-atom insertions) in comparison with the corresponding original compound (black curve).

27.6%–37.3% (7.7%–17.6%) considering the single and the triple Si-atoms substituted configurations. For what concerns the dominant peak the variation is included in the range of about −7.2%–6.3% (−4.3%–10.8%), in the case of coronene (ovalene). Finally, analyzing the exciton-binding energies (E_{bind}) deviations take place for both the molecules around +13.9%–24.4% for coronene and +0.4%–1.5% for ovalene, respectively.

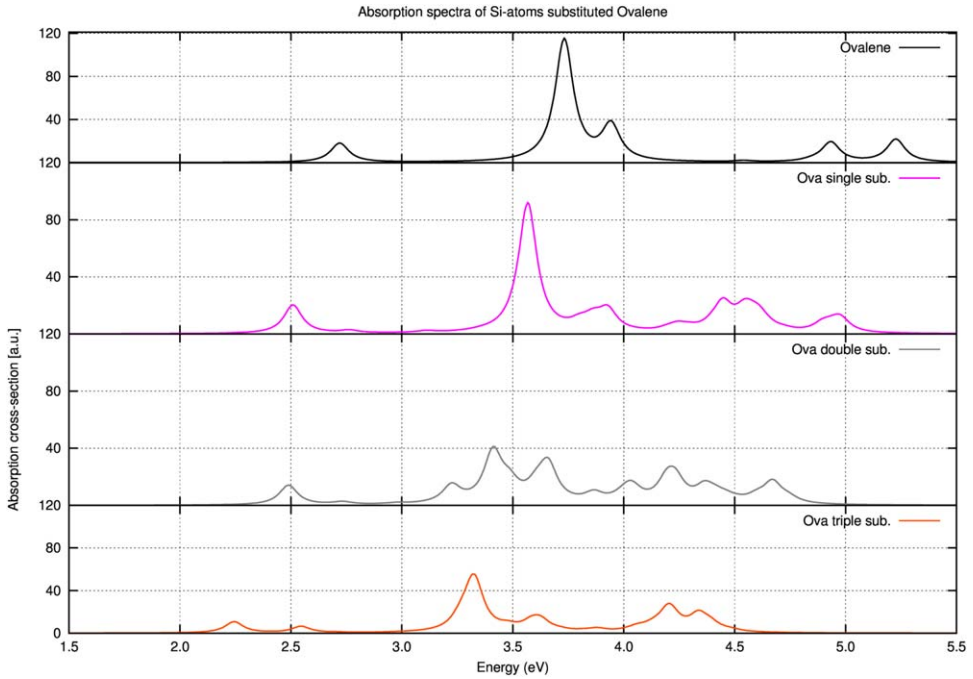

Figure 7. Absorption cross-sections [a.u.] of the selected ovalene substituted systems (with single, double and triple Si-atom insertions) in comparison with the corresponding original compound (black curve).

Table 5. Dominant peaks positions (in wavelength) in the cross-sections of coronene and ovalene after the present calculations and in the experimental absorbance for graphene after [32].

	λ (nm)
Coronene	300
Ovalene	340
Graphene	275

Table 6. Optical onset (E_{opt}), exciton binding energy (E_{bind}) and the energy corresponding to the main peak in the absorption spectrum for coronene and ovalene substituted molecules (with single, dimer and trimer substitution). The percentage deviation, Δ, passing from coronene to ovalene corresponding cluster is also reported.

	E_{opt}	E_{bind}	Dominant peak
Coronene	4.16	2.66	4.16
Single-sub.	3.01	3.31	3.86
Dimer-sub.	2.87	3.19	3.62
Trimer-sub.	2.61	3.03	3.48
Ovalene	2.72 (−35%)	2.68 (+0.8%)	3.73 (−10%)
Single-sub.	2.51 (−17%)	2.65 (−20%)	3.57 (−8%)
Dimer-sub.	2.49 (−13%)	2.64 (−17%)	3.41 (−6%)
Trimer-sub.	2.24 (−14%)	2.69(−11%)	3.33 (−4%)

Table 7. Singlet-singlet lowest-lying permitted excitation energies (eV) of pure and substituted coronene and ovalene as obtained by TDDFT. The corresponding oscillator strengths (O.S.) are given. Each excitation is given in terms of the occupied and virtual molecular orbitals contributing significantly to it (with the corresponding weight in brackets).

	E_{opt}	O.S.	Transition
Coronene	4.16	0.66	$H \rightarrow L$ (0.5)
Single-sub.	3.01	0.03	$H \rightarrow L+1$ (0.56)
Dimer-sub.	2.87	0.06	$H \rightarrow L$ (0.72)
Trimer-sub.	2.61	0.06	$H \rightarrow L$ (0.76)
Ovalene	2.72	0.16	$H \rightarrow L$ (0.92)
Single-sub.	2.51	0.18	$H \rightarrow L$ (0.94)
Dimer-sub.	2.49	0.14	$H \rightarrow L$ (0.88)
Trimer-sub.	2.24	0.13	$H \rightarrow L$ (0.92)

In detail, from figure 5 we can observe that coronene absorption spectrum presents two principal peaks: the main one, which corresponds to the optical onset (E_{opt}), falls at 4.16 eV and an other transition at 6.14 eV, both in the UV range. On the other hand, in the case of ovalene, more peaks appear in the same range. In particular, the ovalene optical onset is separated by the dominant peak and it is redshifted by 1.44 eV with respect to coronene onset, with the main structure located at 3.73 eV. Therefore, ovalene starts the absorption in the visible region, rather than in the UV range, as coronene.

For the modified systems, we have found that, for all the type of substitutions (single, dimer, trimer ones), the insertion of silicon atom/s has as general relevant effect the redshift of either the optical onsets and the dominant peaks. Consequently, each modified compound presents a redshift of its optical absorption range and a redistribution of absorption structures in the UV. With respect to the corresponding substitution, the redshift of the absorption spectra, relative to the main peak, either for coronene and ovalene is of the order of about 10%. We have also found that for one of the trimer-substituted clusters, either for ovalene and coronene, the absorption edge takes place in the IR (at ∼1 eV) (see the appendix for more details).

The global general tendency in the substituted molecules spectra is a reduction of the peaks amplitude, associated with a redistribution of the intensity in the considered range and a greater variety and richness as compared to the pure systems. The more consistent analogy between coronene and ovalene is that all the Si-substituted clusters show the optical absorption more concentrated in the UV, rather than in the visible. Moreover, a significant consequence after silicon insertions is represented by a translation of the optical absorption structure for the substituted systems with respect to their pure counterparts towards the visible. In particular, for both substituted coronenes and ovalenes, silicon insertions give rise to a redshift of the absorption onset as predicted by the fundamental gap reduction reported by ΔSCF calculations [18] (see table 2).

3.3.1. Details of the optical transitions

In this section we reported the details linked to the optical transitions as previously presented, focusing the attention on the nature of the optical onset and the main peak of each original and substituted selected system. The results, that came from the TDDFT calculations, are displayed in tables 7 and 8. For each optical structure it is possible to give information about the transition intensity (quantified by the 'oscillator strength'), the transition weight (that indicates which is the dominant transition), the type of the transition itself (e.g an HOMO–LUMO transition) and the specification of the polarization along a determined spatial coordinate [6]. In tables 7 and 8 'H' indicates the HOMO-level, while 'L' the LUMO-one. If we use the same notation as in [33] the π orbitals involved in the electronic transitions are numbered as a function of the increasing energies: π_{-1}, $\pi_0(\pi_0^*)$ and π_1^* denote respectively, the highest doubly occupied π orbital, the singly occupied (unoccupied) π orbital and the lowest doubly unoccupied π orbital. Based on this notation the HOMO level (H) will be indicated by π_0, while the LUMO (L) one by π_0^* and the other transition states will follow the natural numeration order subscripted, that is: $\pm 1, 2, 3$.

For what concerns the optical onsets, all the transitions involve an excitation of the HOMO–LUMO states with a polarization along the *x* axes of the reference system, that corresponds to the longitudinal one among the three principal symmetry axis of the molecule (see figure 2). In fact, in general, the onset transition involves the HOMO–LUMO levels (see [30]). On the contrary, for the main peaks a greater variety for the states is involved in the corresponding transitions (see table 8). With respect to the optical onsets, all the dominant peaks of the systems under study show larger values of the oscillator strengths, that are reflected in a greater amplitude of the peaks, as is observable in the absorption spectra (see tables 7 and 8 and the appendix for more details).

Table 8. Main peaks (M.P.) of pure and substituted coronene and ovalene as obtained by TDDFT. The corresponding oscillator strengths (O.S.) are given. Each main transition is given in terms of the occupied and virtual molecular orbitals contributing significantly to it with the corresponding weight in brackets.

	M. P. (eV)	O.S.	Transition
Coronene	4.16	0.66	$H \rightarrow L$ (0.5)
Single-sub.	3.86	0.52	$H-1 \rightarrow L+1$ (0.59)
Dimer-sub.	3.62	0.47	$H-1 \rightarrow L+2$ (0.67)
Trimer-sub.	3.48	0.44	$H-1 \rightarrow L$ (0.43)
Ovalene	3.73	1.03	$H-1 \rightarrow L$ (0.45)
Single-sub.	3.57	0.8	$H-1 \rightarrow L$ (0.53)
Dimer-sub.	3.41	0.4	$H-2 \rightarrow L$ (0.21)
Trimer-sub.	3.33	0.5	$H-2 \rightarrow L$ (0.41)

4. Conclusions

We have presented a systematic comparative investigation on the electronic and optical properties of coronene and ovalene molecules in their unsubstituted and substituted forms: with individual silicon atoms, Si-dimers and Si-trimers. In the framework of DFT and TDDFT computational schemes, we have computed electron affinities, ionization energies, fundamental gaps, optical onset energies and absorption spectra. We have found larger values of the ground-state energies for all the substituted configurations with respect to the original counterparts. In both coronene and ovalene molecules, we recorded a general reduction of the fundamental gap and optical onset energies as a consequence of the chemical modification.

Concerning the optical properties, for each type of substitution, the absorption spectra show a redshift of the optical onsets and a remodeling of the main peaks intensity. In addition, in one case of Si-trimer substitution, for both coronene and ovalene, the absorption edge takes place in the IR (at ∼1 eV), rather than the in visible (ovalene) or in the UV (coronene). The present evaluation of the effects of Si-atoms substitutions, on the electronic and optical properties of the two first Circumacenes members, could help in the choice of the best substitutional path to be found to enhance specific excitation properties of these molecules for different applications in optoelectronic devices.

Acknowledgments

P M gratefully acknowledges Sardinia Regional Government for the financial support of her PhD scolarship (POR Sardegna FSE Operational Programme of the Autonomous Region of Sardegna, European Social Fund 2007.201 3 -Axis IV Human Resources, Objective I.3, Line of Activity I.3.1). GC and RC acknowledge partial financial support from IDEA-AISBL Bruxelles. GC acknowledges moreover partial financial support from 'Progetto biennale d'Ateneo UniCa/FdS/RAS (Legge Regionale 7 agosto 2007, n. 7annualita'; 2016) - Multiphysics theoretical approach to thermoelectricity'.

Appendix

In this section we have reported the computed absorption spectra of all the systems in exam: i.e. for both coronene and ovalene, all the allowed configurations with single, dimer and trimer Si-substitutions with the corresponding ground-state energy value, as obtained after DFT calculations. In figures A1–A6 the *y*-axes give the peak amplitude representation, each cluster is identified by a number and the corresponding pure parent is represented by a black curve on the top of each plot. In addition to this, the numbers corresponding to the configuration selected for the stability from the energetic point of view are 0, 3 and 2 (7, 7, 6) respectively for single, double and triple coronene (ovalene) substituted systems (see the main text for explanations and the corresponding tabulated energy value). From table A1 in the case of coronene, the energy differences (in absolute value) between the most and the less stable configurations are of about 1.9, 5.5 and 3.6 eV, for single, dimer and trimer-substitued systems. It follows that the energy variations, calculated with respect the original parent, oscillate between 6.337–6.339 keV, 13.673–13.678 keV and 20.514–20.518 keV, for single, dimer and trimer substitutions, respectively. While considering ovalene, according to table A2, we have recordered that the energy differences (in absolute value) between the most and the less stable configurations are of about 3.2, 2.7 and 3.4 eV, for single, dimer and trimer-substitued systems. Moreover, the energy variations, calculated

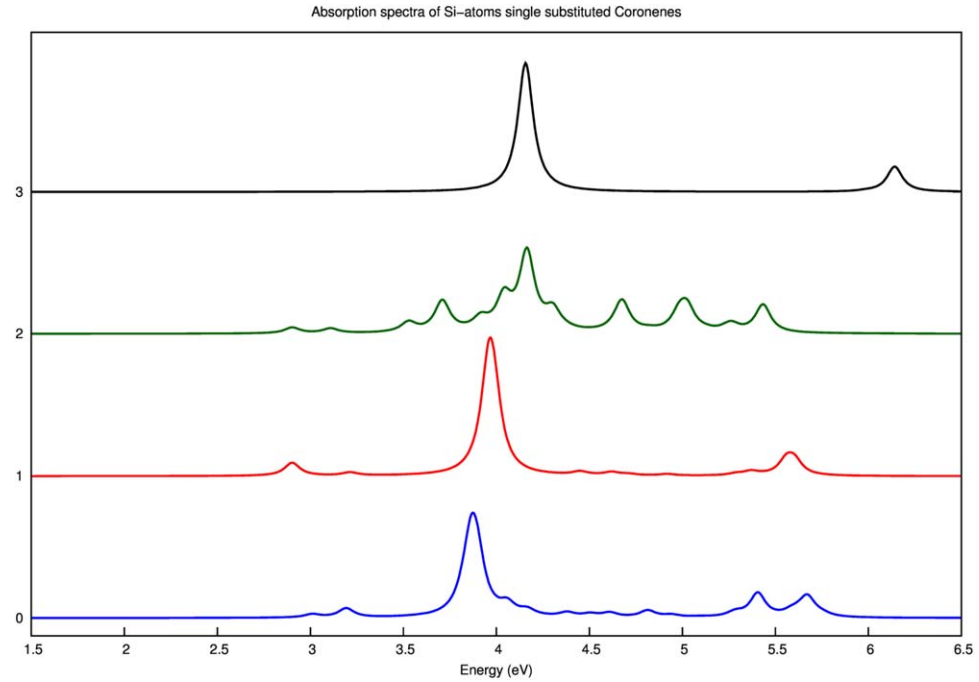

Figure A1. Computed absorption cross-sections [a.u.] for coronenes with an individual Si-atom substituted (from 0 to 2), while the curve relative to the original molecule is at the top (black one).

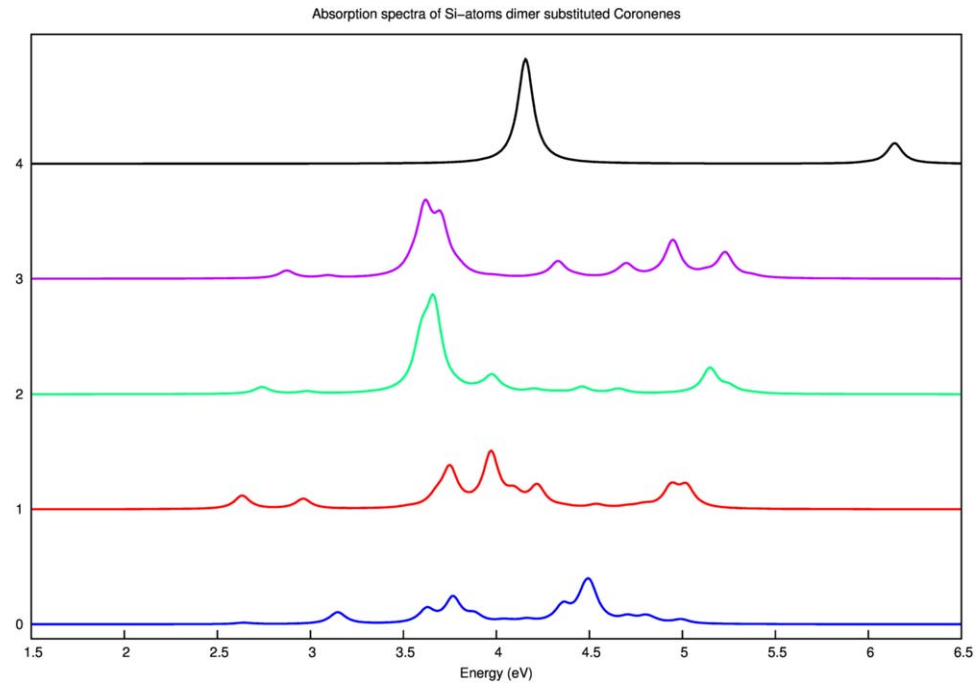

Figure A2. Computed absorption cross-sections [a.u.] for coronenes with a dimer of Si-atom substituted (from 0 to 3), while the curve relative to the original molecule is at the top (black one).

with respect the original molecule, oscillate between 6.836–6.839 keV, 13.675–13.678 keV and 20.515–20.518 keV, for single, dimer and trimer substitutions, respectively. The detailed description for each individual plot will be followed by a comment on the general trend. For the details related to the different configurations, tables A1 and A2 report the corresponding atomic positions and the composition for single atom, dimers and trimers of each substituted cluster, with the letters as indicated in figure 1, for coronene and ovalene, respectively.

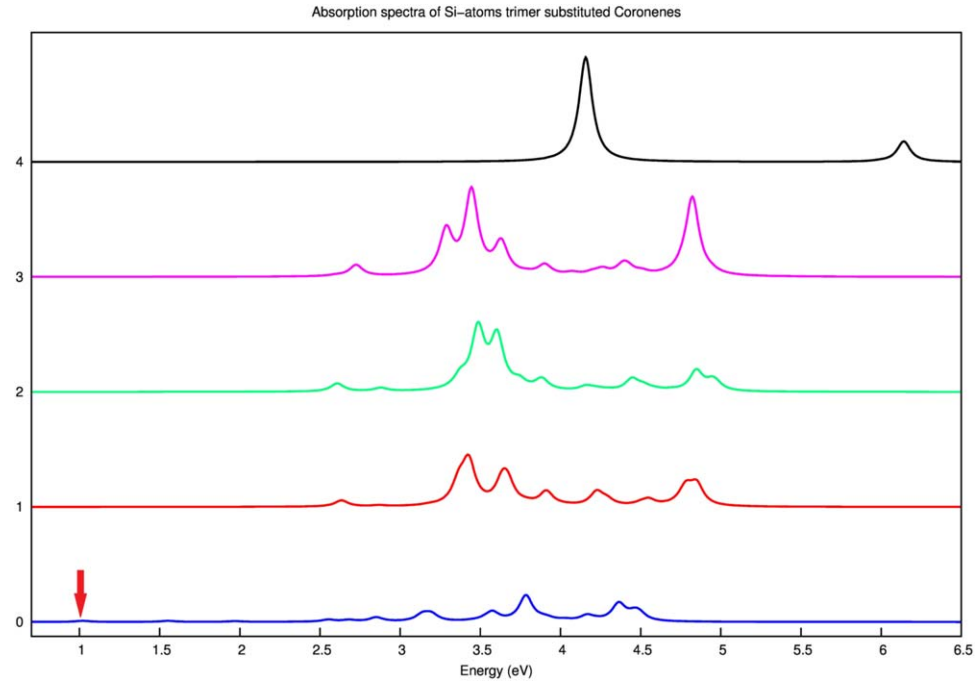

Figure A3. Computed absorption cross-sections [a.u.] for coronenes with a trimer of Si-atom substituted (from 0 to 3), while the curve relative to the original molecule is at the top (black one). The red arrow indicates the only case, for the trimer-substitued configurations, in which the onset position is placed in the IR.

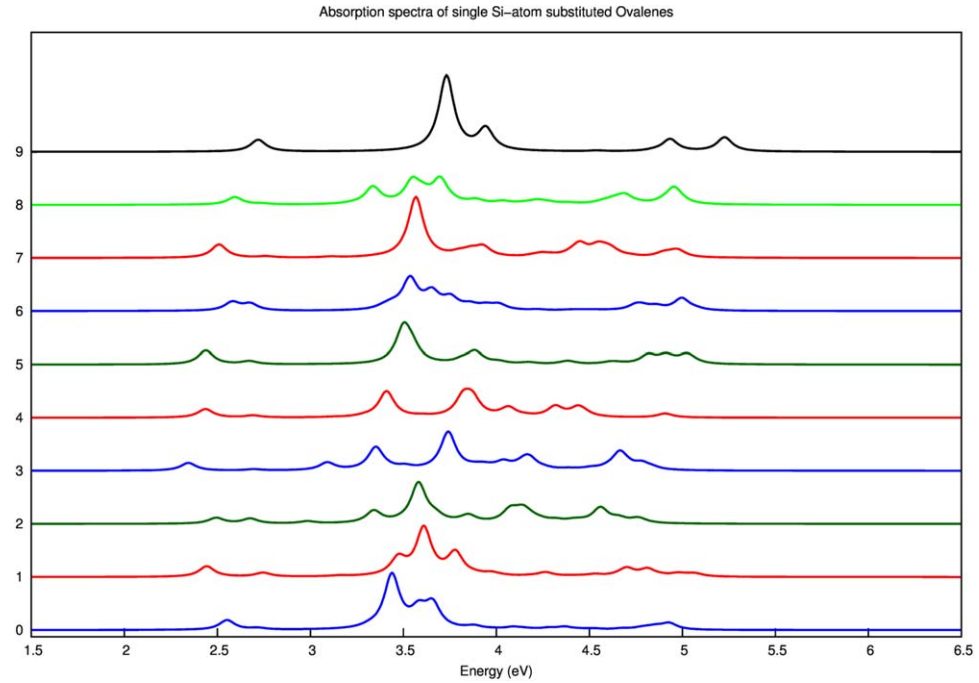

Figure A4. Computed absorption cross-sections [a.u.] for ovalenes with an individual Si-atom substituted (from 0 to 8), while the curve relative to the original molecule is at the top (black one).

For single-substituted coronenes (see figure A1), a redshift either for the dominant peaks (apart from the system labeled by number 2) and all the optical onsets with respect to their original parent takes place (with an average shift value of about 10% and 25% for the main peaks and the onsets, respectively). This fact is true also for the double and the triple substitutions (see figures A2 and A3), with in addition the presence of a split in the main peak's structure, accompanied by a gradual loss in amplitude. Only in the case of the configuration

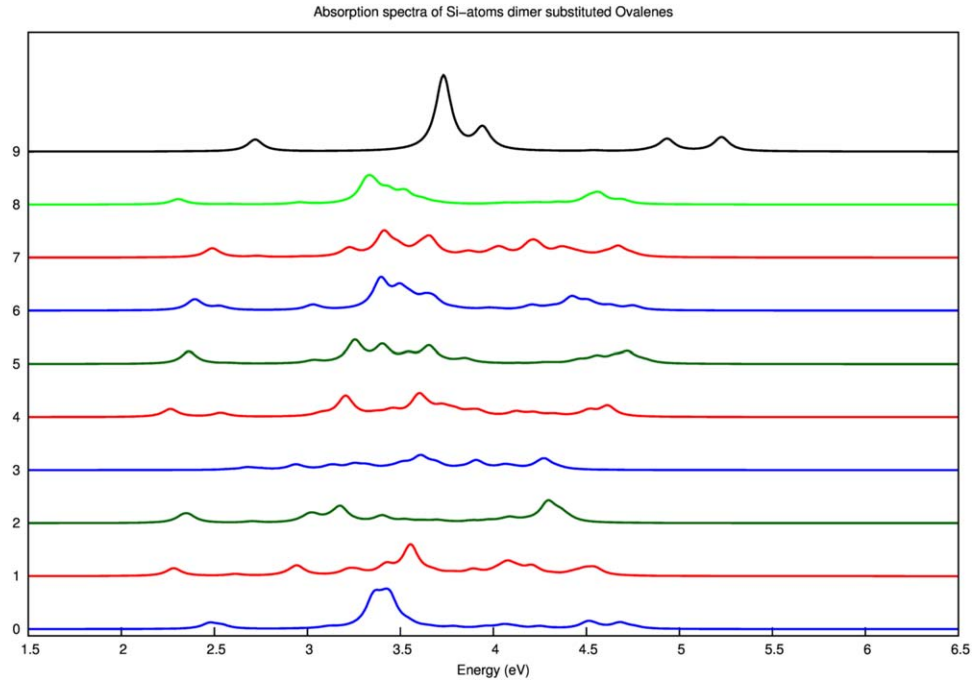

Figure A5. Computed absorption cross-sections [a.u.] for ovalenes with a dimer of Si-atom substituted (from 0 to 8), while the curve relative to the original molecule is at the top (black one).

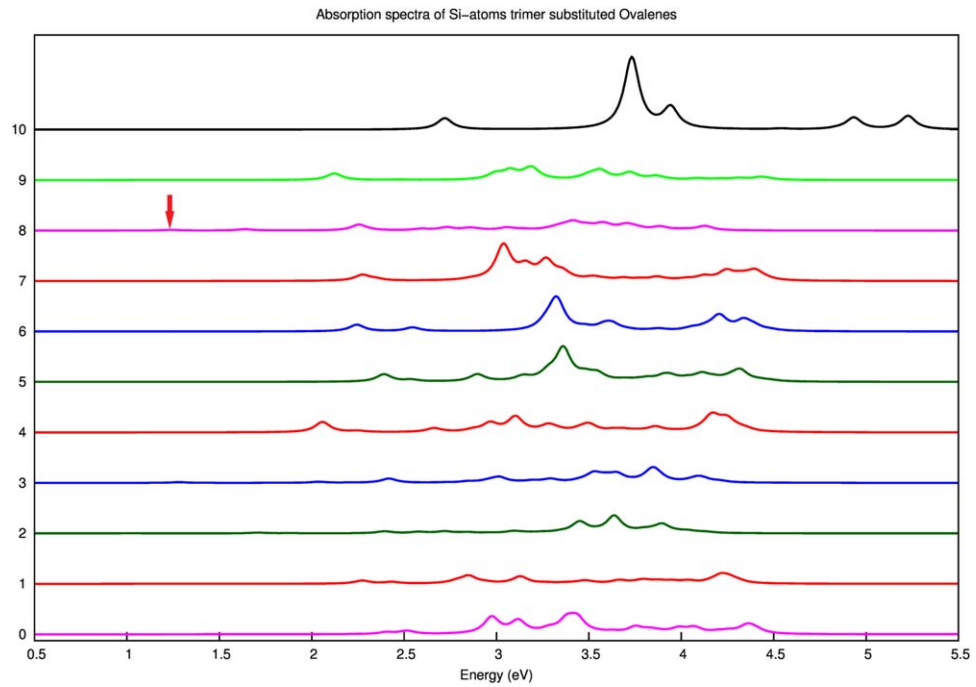

Figure A6. Computed absorption cross-sections [a.u.] for ovalenes with a trimer of Si-atom substituted (from 0 to 9), while the curve relative to the original molecule is at the top (black one). The red arrow indicates the only case, for the trimer-substitued configurations, in which the onset position is placed in the IR.

indicated by number 0, for double substitutions, the main peak is blue-shifted with respect to the pure coronene (with blueshift of 0.3 eV).

In particular, concerning trimer-substituted coronenes, the absorption spectrum is characterized by a nearly regular alignment of the optical onsets around 2.7 eV, with the exception of trimer 0, whose onset falls in the IR region. In this case the onset redshift is consistent and of the order of ~75%, passing from 4.16 eV (coronene) to

Table A1. Correspondence table for the curves' number in the absorption spectra (see figures A1–A3) and the atomic position, indicated by letters in the clusters (see figure 1), for single, double and triple substituted coronenes. For each system the corresponding ground-state energy value (eV) on which is based the selection criterion is also reported.

Curve	Single	(eV)	Dimers	(eV)	Trimers	(eV)
0	A	−31423.77	CD	−38757.73	CDG	−45599.34
1	B	−31423.72	DE	−38761.18	CBA	−45601.99
2	C	−31421.87	EF	−38763.04	BAF	−45602.96
3	Coronene	−25084.84	AF	−38763.22	EFH	−45602.11
4	—		Coronene	−25084.84	Coronene	−25084.84

Table A2. Correspondence table for the curves' number in the absorption spectra (see figures A4–A6) and the atomic position, indicated by letters in the clusters (see figure 1), for single, double and triple substituted ovalenes. For each system the corresponding ground-state energy value (eV) on which is based the selection criterion is also reported.

Curve	Single	(eV)	Dimers	(eV)	Trimers	(eV)
0	A	−40253.06	AB	−47092.37	ABC	−53931.29
1	B	−40253.03	BC	−47090.47	BCD	−53930.55
2	C	−40251.17	CD	−47089.85	CDE	−53928.84
3	D	−40251.14	DE	−47089.86	EDG	−53929.50
4	E	−40250.67	DG	−47090.37	FGH	−53931.14
5	F	−40252.95	FG	−47092.07	GHI	−53932.03
6	G	−40252.89	GH	−47092.08	HIB	−53932.26
7	H	−40253.92	HI	−47092.55	IBA	−53931.38
8	I	−40253.06	IB	−47091.65	CDG	−53929.30
9	Ovalene	−33414.13	Ovalene	−33414.13	DGF	−53931.19
10	—		—		Ovalene	−33414.13

1.02 (system 0). The onsets' alignment arises also in the case of single and double-substituted ovalene, with a gradual loss of the alignment order and a larger decrease of the peaks amplitude. In these cases, the absorption structures are variegated and different from each other. The situation becomes different for the trimer-substituted ovalenes because the optical onsets' alignment is globally lost and each main peak is characterized by a reduction of its amplitude. In particular, for ovalene trimer-substituted spectra (see figure A6) the decrease of peaks amplitude aside from 5 to 7 cases is dramatic and one might expect that the trend could continue increasing the number of silicon atoms substitutions.

One can consider as a general trend, valid for each type of insertion, that a redshift of the optical onsets takes palce for each substituted system: the redshift increases according to the number of inserted silicon atoms. Moreover, in one case, for both coronene and ovalene trimer-substituted configuration, we have found that the optical onset is placed at around 1 eV, in the IR. This is the case of the system labeled by number 0 (8) for coronene (ovalene), while the onset point is indicated by the red arrow in figures A3 and A6.

For what concerns the main peak behavior for ovalenes, in some substituted systems spectra, the dominant peak is separated in two or more different curves, redistributed in several structures between 3 and 5 eV, as compared to their original parent. These are, for example, the cases of single-substituted configuration indicated by number 2 (0), the double-substituted system 0 (4) and the trimer-substituted geometry 3 (6) for coronene (ovalene). However, this feature is quite different for coronene, whose modified configurations for the main peak in the absorption spectrum show more localized structures.

The other main tendency, as a consequence of silicon inclusions, is the general attenuation of the intensity in the amplitude of the dominant peaks (verifiable quantitatively through the value of their corresponding oscillator strengths, see table 8) and a remodeling in the spectral profile. Each system tends to show a particular optical behavior and this is valid for each type of substitution, for both coronene and ovalene. The extreme dependence on the Si-atoms substitutional site causes the evident peculiarity of each spectra among the different configurations. This fact demonstrates the strong relationship between the Si-atom substitutional site and the corresponding optical absorption spectrum of the substituted molecule: aside from the above discussed general trends, there is, in fact, one correspondence between Si-atoms substitutional site and corresponding optical spectrum of the substituted clusters; the spectra therefore turn out to be different from each other.

References

[1] Andre K G 2011 *Rev. Mod. Phys.* **83** 851–62
[2] Lin C-L, Arafune R, Kawahara K, Tsukahara N, Minamitani E, Kim Y, Takagi N and Kawai M 2012 *Appl. Phys. Express* **5** 1–3
[3] Soref R A 1993 *Proc. IEEE* **81** 1687–706
[4] Dimuthu K L, Weerawardene M and Aikens C M 2015 *J. Phys. Chem. Lett.* **6** 3341–5
[5] Malloci G, Cappellini G, Mulas G and Mattoni A 2011 *Chem. Phys.* **384** 19–27
[6] Cardia R, Malloci G and Cappellini G 2016 *SPIE Photonics VII Conf. Proc.* vol 9895, p 8
[7] Perez-Jimenez A J and Sancho-Garcia J C 2009 *Nanotechnology* **20** 47
[8] Jennings E, Montgomery W and Lerch P 2010 *J Phys. Chem.* B **114** 1575–8
[9] Zhou W, Lee J, Nanda J, Pantelides S T, Pennycook S J and Idrobo J-C 2012 *Nat. Nanotechnol. Lett.* **7** 161–5
[10] Matthes L, Gori P, Pulci O and Bechstedt F 2013 *Phys. Rev.* B **87** 035438
[11] Zhou W, Kapetanakis M D, Prange M P, Pantelides S T, Pennycook S J and Idrobo J-C 2012 *Phys. Rev. Lett.* **109** 1–5
[12] Kohn W 1999 *Rev. Mod. Phys.* **71** 213–37
[13] Runge E and Gross E K U 1984 *Phys. Rev. Lett.* **52** 997
[14] Becke A D 1993 *J. Chem. Phys.* **98** 5648–52
[15] Lee C, Yang W and Parr R G 1988 *Phys. Rev.* B **37** 785–9
[16] Stephens P J, Devlin P J, Chabalowski C F and Frisch M J 1994 *Phys. Rev.* B **99** 11623–7
[17] Ernzerhof M and Scuseria G E 1999 *J. Chem. Phys.* **110** 5029–36
[18] Cardia R, Malloci G, Mattoni A and Cappellini G 2014 *J. Phys. Chem.* A **118** 5170–7
[19] Cardia R, Malloci G, Rignanese G M, Blase X, Molteni E and Cappellini G 2016 *Phys. Rev.* B **93** 235132
[20] Cappellini G, Malloci G and Mulas G 2009 *Superlattices Microstruct.* **46** 14–8
[21] Jones R O and Gunnarsson O 1989 *Rev. Mod. Phys.* **61** 689–746
[22] Malloci G, Cappellini G, Mulas G and Satta G 2004 *Phys. Rev.* B **70** 1–5
[23] Casida M E 1995 *World Sci.* **1** 155–92
[24] Onida G, Reining L and Rubio A 2002 *Rev. Mod. Phys.* **74** 601
[25] Dardenne N *et al* 2017 *J. Phys. Chem.* C **121** 24480–8
[26] Valiev M *et al* 2010 *Comput. Phys. Commun.* **181** 1477–89
[27] Mocci P, Cardia R and Cappellini G 2018 *J. Phys.: Conf. Ser.* **956** 012020
[28] Lin H *et al* 2008 *Nanotechnology* **19** 325601
[29] Treitel N *et al* 2004 *Phys. Chem. Chem. Phys.* **6** 1113–21
[30] Malloci G, Joblin C and Mulas G 2007 *Chem. Phys.* **332** 353–9
[31] www.nist.gov/srd
[32] Ciplak Z, Yildiz N and Calimli A 2014 *Fullerenes, Nanotubes Carbon Nanostruct.* **23** 361–70
[33] Malloci G, Mulas G, Cappellini G and Joblin G 2007 *Chem. Phys.* **340** 43–58